Facile RAFT synthesis of side-chain amino acids containing pH-responsive hyperbranched and star architectures†

Saswati Ghosh Roy and Priyadarsi De*

This work reports the design and synthesis of amino acid-based hyperbranched polymers *via* the combination of self-condensing vinyl polymerization (SCVP) and reversible addition–fragmentation chain transfer (RAFT) polymerization from *tert*-butyl carbamate (Boc)-L-valine acryloyloxyethyl ester (Boc-Val-HEA) and S-(4-vinyl)benzyl S'-butyltrithiocarbonate (VBBT) with variable degrees of branching (DB), molecular weights (M_n), and chain end functionalities. Copolymerization kinetics reveal that the molecular weight increases and the DB decreases linearly with time as the branch length increases with the conversion of the Boc-Val-HEA monomer. These hyperbranched polymers, P(Boc-Val-HEA-*co*-VBBT), with tuneable M_n and DB have been further employed *via* successive RAFT polymerizations for the synthesis of star polymers with variable arm numbers and lengths. The removal of Boc groups from the polymers results in water soluble pH-responsive cationic hyperbranched architectures with tuneable pH responsiveness, differing from 6.8–7.5 due to the incorporation of various degrees of hydrophobic chain end functionalities with the variation of monomer feed compositions. Dynamic light scattering (DLS), atomic force microscopy (AFM) and scanning electron microscopy (SEM) reveal the interesting self-assembly of the Boc-deprotected star polymers in aqueous media with amino acid-based cores and water soluble thermoresponsive arms. Below the hydrophilic to hydrophobic transition pH and temperature, star polymers remain as unimers in aqueous solution. However, above the transition pH (and below the transition temperature), they form multi-micellar aggregates, which further fuse together to form larger aggregates above the transition temperature.

Introduction

In recent years, significant attention has been paid to the synthesis of polymers with different chain architectures, *e.g.*, linear, grafted, hyperbranched, dendrimers, comb-, brush- and star-shaped with the purpose of studying the structural property correlation in the solution phase or in the bulk state. Among the various architectures, hyperbranched and star polymers are interesting materials due to their several unique properties compared to their respective linear analogues, such as enhanced solubility in a wide range of solvents due to their decreased chain entanglement, low melt and solution visco-

Polymer Research Centre, Department of Chemical Sciences, Indian Institute of Science Education and Research Kolkata, Mohanpur – 741246, Nadia, West Bengal, India. E-mail: p_de@iiserkol.ac.in

sities, reduced hydrodynamic volume, critical phase behaviour, and the presence of a huge number of chain end functionalities available for further chemical modifications.[1] These important characteristics make them very good candidates for a wide range of applications, such as for the modification of materials and resins,[2,3] as a support system for catalysis, as a gene,[4] and in drug delivery devices.[5,6] Generally, hyperbranched polymers are synthesized following three main strategies: (i) step growth polymerization *via* the polycondensation of AB_x type macromonomers,[7,8] (ii) the copolymerization of conventional monomers with divinyl cross-linkers[9,10] or with monomers containing a polymerizable vinyl group and a dormant initiating site/chain transfer functionality (inimer) *via* self-condensing vinyl polymerization (SCVP),[11,12] and (iii) the ring opening polymerization of dormant AB_x macromonomers.[13] Moreover, the reversible activation/deactivation controlled polymerization of multifunctional vinyl monomers can give hyperbranched polymers with a high degree of branching (DB) and numerous vinyl functional groups.[14–16] However, among the abovementioned strategies, SCVP is the most versatile method for the synthesis of hyperbranched polymers.

It was first introduced by Fréchet and co-workers using a conventional monomer and an inimer to achieve control over the degree of branching of the hyperbranched polystyrene and polyacrylates.[17] The combination of SCVP with a controlled/living polymerization, such as nitroxide-mediated radical polymerization,[18] atom transfer radical polymerization[19,20] and reversible addition–fragmentation chain transfer (RAFT) polymerization has been efficiently employed for the synthesis of hyperbranched and star polymers with controlled branch lengths and variable functionalities. Among these, RAFT is the most versatile technique for the synthesis of macromolecules due to the mild reaction conditions, and tolerance to a high degree of monomer functionalities and solvents.[21]

Thus, RAFT has been employed to synthesize various ranges of hyperbranched polymers using divinyl comonomers,[22] pendant xanthate co-monomer groups,[23] and AB*-type chain transfer agents (CTA).[24] Rimmer and coworkers synthesized a series of thermo-responsive hyperbranched polymers using imidazole-based polymerizable CTA with trithiocarbonate functionality.[25] Sumerlin's group synthesized poly(N-isopropyl acrylamide) based thermo-responsive hyperbranched polymers using acryloyl trithiocarbonate CTA.[26] In both cases, the solution property of thermo-responsive hyperbranched polymers is greatly influenced by the end group's polarity and DB. To date, to the best of our knowledge, the influence of DB on the solution behaviour of pH-responsive hyperbranched polymers prepared via SCVP-RAFT has not been explored. Therefore, the synthesis and study of pH-responsive cationic hyperbranched polymers is an interesting research area because of their cationic nature, which may make them interesting and competitive candidates with respect to linear and branched polyethyleneimine (PEI) for non-viral gene delivery. PEIs are widely explored synthetic cationic polymeric carriers for the plasmid DNA (pDNA) to cells due to the high transfection efficiency of PEI/pDNA complexes.[27] However, the major drawback associated with the PEI-based delivery systems is their toxicity, due to the strong positive surface charge as branched PEIs are composed of multiple cationic primary, secondary and tertiary amine groups.[28] Thus, it would be interesting to prepare hyperbranched polymers with pendant naturally occurring amino acid moiety with only primary amine groups at the surface of the polymers, as these are expected to be less toxic compared to PEI[29] and could be employed as alternative and efficient gene delivery devices.

In the last few decades, the incorporation of naturally occurring amino acid moiety into synthetic polymers has become an interesting research area,[30,31] because the inclusion of an amino acid moiety increases the water solubility, enhances biocompatibility, and instigates a higher order hierarchical structure through non-covalent interactions like H-bonding, electrostatic interactions, and hydrophobic stacking.[32,33] Recently, Sun and Gao reported L-phenylalanine, glycine, L-alanine, L-valine, and L-lysine based cationic polyelectrolytes with low cytotoxicity and excellent DNA binding capability.[29] Our group recently reported pH-responsive cationic polyelectrolytes with controlled molecular weight and narrow polydispersity via RAFT technique from (meth)acrylate-containing side-chain amino acid-based chiral monomers, such as L- and D-tryptophan,[34] L-alanine, L-phenylalanine,[35] L-leucine and L-isoleucine.[36] Therefore, the SCVP-RAFT of amino acid-based monomers can produce pH-responsive hyperbranched polymers with remarkable structures and aqueous solution properties. In this work, we have synthesized tert-butyl carbamate (Boc)-L-valine acryloyloxyethyl ester (Boc-Val-HEA) and employed it in SCVP-RAFT copolymerization with a monomer CTA, S-(4-vinyl)benzyl S′-butyltrithiocarbonate (VBBT) using various co-monomer feed ratios to afford hyperbranched copolymers with variable DB and CTA functionalities, which can be further exploited for the synthesis of star polymers with branched cores via successive RAFT polymerization reactions. The Boc group deprotection from hyperbranched and star architectures results in water soluble polymers with tuneable pH-responsive properties with the variation of DB due to the presence of various degrees of chain end functionalities.

Experimental section

Materials

Boc-L-valine (Boc-L-Val-OH, 99%), and trifluoroacetic acid (TFA, 99.5%) were purchased from Sisco Research Laboratories Pvt. Ltd., India and used as received. 4-Dimethylaminopyridine (DMAP, 99%), dicyclohexylcarbodiimide (DCC, 99%), 2-hydroxyethyl acrylate (HEA, 97%), 4-vinylbenzyl chloride (90%), sodium methoxide (95%), 1-butanethiol (99%), anhydrous N,N-dimethylformamide (DMF, 99.9%) and anhydrous methanol (99.9%) were purchased from Sigma and used without any further purification. The 2-(2-methoxyethoxy)ethyl methacrylate (MEO$_2$MA, 95%) and polyethylene glycol methyl ether methacrylate (PEGMA, M_n = 300 g mol^{-1}, 98%) were purchased from Sigma, and purified by passing them through a basic alumina column prior to polymerization. 2,2′-Azobis-isobutyronitrile (AIBN, Sigma, 98%) was recrystallized twice from methanol. CDCl$_3$ (99.8% D), CD$_3$OD (99.8% D), and D$_2$O (99.8% D) was purchased from Cambridge Isotope Laboratories, Inc. for the NMR studies. The solvents, such as hexanes, acetone, ethyl acetate, dichloromethane (DCM), and tetrahydrofuran (THF), were purified following the standard procedures.

Methods

The molecular weights and molecular weight distributions (polydispersity index, PDI) of the polymers were determined by gel permeation chromatography (GPC). Details about the GPC analysis, ^{1}H NMR study, UV-Vis spectroscopic measurements, dynamic light scattering (DLS), differential scanning calorimetry (DSC), and the positive mode electrospray ionization mass spectrometer (ESI-MS) can be found elsewhere.[36] Atomic force microscopy (AFM) imaging experiments were performed on a NT-MDT NTEGRA Prima Scanning Probe Microscope. A field-emission scanning electron microscopic

(FE-SEM) study was carried out with a Carl Zeiss-Sigma instrument.

Synthesis of monomer

The Boc-Val-HEA was synthesized by the esterification coupling reaction of Boc-Val-OH with HEA in the presence of DCC and DMAP. The Boc-Val-OH (10.00 g, 46.03 mmol) was dissolved in 150 mL ethyl acetate in a 500 mL double-necked round bottom flask containing a magnetic stir bar and purged with dry N_2 gas for 20 min. Then, DCC (50.63 mmol, 10.45 g) in 50 mL ethyl acetate was added dropwise, followed by the addition of DMAP (2.30 mmol, 0.28 g) with constant stirring. The reaction vessel was maintained in an ice-water bath, and HEA (46.03 mmol, 5.34 g) was added dropwise for 15 min. The ice-water bath was removed after 30 min, and the reaction mixture was stirred at room temperature for 24 h. The reaction mixture was filtered to eliminate insoluble N,N'-dicyclohexylurea (DCU) and the filtrate was washed successively with 0.1 N HCl (200 mL × 4), concentrated $NaHCO_3$ (200 mL × 4) and brine solution and dried over anhydrous Na_2SO_4 overnight. The filtrate was concentrated on a rotary evaporator and the resultant viscous liquid was purified by column chromatography, using ethyl acetate–hexanes (1 : 6) as the mobile phase to yield 12.2 g (79.7%) pure colourless viscous liquid. ^{1}H NMR (Fig. S1,† $CDCl_3$, δ, ppm): 6.46–6.39 and 5.88–5.83 (HC=CH_2, 2H, d), 6.16–6.08 (HC=CH$_2$, 1H, m), 5.02 (NH–COO, 1H, s), 4.48–4.39 (–O–CH_2–CH_2–O–, 4H, m), 4.24 (NH–CH–CO, 1H, d), 2.14 (CHMe$_2$, 1H, m), 1.44 (–CMe_3, 9H, s), 0.97–0.86 (CHMe_2, 6H, d). ^{13}C NMR (Fig. S2,† $CDCl_3$, δ, ppm): 172.01 (–OOC–CH$_2$–CH$_2$–), 165.64 (H$_2$C=CH–CO–), 155.47 (–NH–COO–), 131.33 (H$_2$$C$=CH–), 127.94 (H$_2$C=$C$H–), 79.66 (–$CMe_3$), 62.71 & 61.84 ((–O–$CH_2$–$CH_2$–O–), 58.45 (NH–$C$H–CO), 31.33 (–$CMe_2$), 28.40 (–C($CH_3$)$_3$), 19.05 & 17.36 (C($CH_3$)$_2$). FT-IR (cm^{-1}): 3377 (N–H), 2970, 2935 and 2877 (C–H), 1726, (C=O), 1636 (C=C), 1503 (N–H), 1458, 1367, 1296, 1273, 1246, 1178, 1158 (C–O), 1077, 1045, 984, 870, 810. ESI-MS: $[M + Na^+]$ = 338.16 m/z (Fig. S3†).

Synthesis of S-(4-vinyl)benzyl S′-butyltrithiocarbonate (VBBT) CTA

1-Butanethiol (6.00 g, 67.0 mmol) in 30 mL of anhydrous methanol was placed in a 250 mL round-bottomed flask and a solution of sodium methoxide (3.63 g, 67.30 mmol) in 50 mL methanol was added dropwise under a nitrogen atmosphere. The reaction mixture was stirred for 2 h and CS$_2$ (6.31 g, 83.0 mmol) was added dropwise to the solution with further stirring at room temperature for 5 h. 4-Vinylbenzyl chloride (10.2 g, 67.0 mmol) was added dropwise to the yellow coloured reaction mixture, and the solution was stirred overnight under a nitrogen atmosphere. 250 mL of de-ionized (DI) water was added to the reaction mixture followed by extraction with DCM (200 mL × 5), and the combined organic layer was dried over anhydrous Na_2SO_4 overnight. The solvent was removed under reduced pressure and the crude product was purified by column chromatography using hexane as the mobile phase to obtain pure VBBT (12.7 g, 73.4% yield) as a yellow viscous oil.

^{1}H NMR (Fig. S4,† $CDCl_3$, δ, ppm): 6.73–6.65 (CH$_2$=CH, 1H, m), 5.75–5.70 and 5.26–5.22 (CH_2=CH, 2H, d), 7.38–7.25 (C$_6H_4$, 4H, m), 4.59 (Ar–CH_2, 2H, s), 3.40–3.35 (S–CH_2, 2H, t), 1.72–1.65 (S–CH$_2$–CH_2, 2H, m), 1.48–1.38 (CH$_3$–CH_2, 2H, m), 0.96–0.90 (CH_3, 3H, t). ^{13}C NMR (Fig. S5,† $CDCl_3$, δ, ppm): 223.49 (–S–(C=S)–S–), 137.13, 136.10, 129.23 and 126.54 (–C_6H_4–, f, c, d, e carbon, respectively), 134.50 (H$_2$C=CH–), 114.41 (H$_2$$C$=CH–), 41.28 (–$C_6H_4$–$CH_2$–), 36.52 (–S–$CH_2$–), 30.18 (–S–CH$_2$–$CH_2$–), 22.22 (–S–CH$_2$–CH$_2$–$CH_2$–), 13.74 (–$CH_2$–$CH_3$). FT-IR (cm^{-1}): 3085 (=C–H), 2958, 2926, 2870 (C–H), 1629 (C=C, alkene), 1510, 1442 (C=C, Ar), 1405 (C–H), 1053 (C=S), 772 (C–S). ESI-MS: $[M^+]$ = 282.29 m/z (Fig. S6†).

Synthesis of hyperbranched copolymers of Boc-Val-HEA and VBBT by RAFT copolymerization

The RAFT copolymerization of Boc-Val-HEA with VBBT was carried out in DMF using AIBN as a radical source at 70 °C, where VBBT acted both as CTA, as well as the polymerizable monomer. Typically, Boc-Val-HEA (0.5 g, 1.585 mmol), VBBT (89.6 mg, 0.317 mmol), AIBN (5.2 mg, 31.7 μmol), 0.5 g DMF and a small magnetic stir bar were taken in a 20 mL septa-sealed glass vial. The reaction vial was purged with dry nitrogen for 20 min, and the polymerization was carried out in a preheated reaction block at 70 °C. The polymerization was quenched after a predetermined time by cooling the reaction mixture in an ice-water bath, followed by exposure to air. The monomer conversion was determined by ^{1}H NMR spectroscopy by comparing the peak areas between the vinyl proton (6.16–6.08 ppm) of the monomer at time zero and at the final time with respect to the DMF solvent resonance peak at 8.02 ppm. The reaction mixture was diluted with acetone and precipitated into hexane. The resultant polymer was collected as a yellow powder after repeated precipitation of the polymer solution in acetone (solvent) from hexane (nonsolvent), and then dried under a high vacuum for 6 h. To study the kinetics of the RAFT polymerization, an aliquot (~0.1 mL) was withdrawn from the reaction vial using a N_2-purged syringe at predetermined time intervals. The reaction mixtures were analyzed by ^{1}H NMR and GPC to determine the monomer conversion, the DB, the number average molecular weights ($M_{n,GPC}$) and the PDI.

Synthesis of linear homopolymer of Boc-Val-HEA *via* RAFT polymerization

Boc-Val-HEA (0.20 g, 0.63 mmol), 4-cyano-4-(dodecylsulfanylthiocarbonyl)sulfanylpentanoic acid (CDP) (5.11 mg, 0.013 mmol), AIBN (0.21 mg, 0.0013 mmol; from AIBN stock solution), 0.6 g DMF and a magnetic stir bar were placed in a 20 mL septa-sealed glass vial, purged with dry N_2 for 20 min, and then placed in a preheated reaction block at 70 °C for 5 h. The resultant polymer was purified following the same procedure as discussed above for hyperbranched polymers to yield (71%) a yellowish powder.

Synthesis of star polymers with hyperbranched cores *via* RAFT polymerization

First, a low molecular weight hyperbranched macro-chain transfer agent (macro-CTA) was synthesized from Boc-Val-HEA and VBBT. The purified P(Boc-Val-HEA-*co*-VBBT) macro-CTA (M_n = 8200 g mol^{-1}, PDI = 1.38, 91.11 mg, 11.11 μmol), PEGMA (0.5 g, 1.67 mmol), AIBN (0.18 mg, 1.11 μmol; from stock solution), and 1.58 g anhydrous DMF were charged in a 20 mL septa-sealed vial. The vial was purged with dry N$_2$ for 20 min and polymerization was carried out under stirring at 70 °C for 230 min. After quenching the polymerization, purification of the polymer was carried out following the same procedure as described in the previous section. The monomer conversion was determined by gravimetric analysis by comparing the amounts of the final polymers with respect to the monomers in the feed.

Boc group deprotection

Typically, 250 mg polymer was dissolved in 1.5 mL TFA in a 20 mL glass vial and stirred for 1 h at room temperature. Subsequently, Boc-deprotected polymers were isolated by washing with a large volume of hexanes followed by reprecipitation from diethyl ether (×3) before being dried under high vacuum for 12 h to obtain a yellowish powder (yield: ~90%).

Morphology study of star polymers by AFM and SEM

To study the pH-induced aggregation and self-assembly behaviour of various star polymers by AFM and SEM experiments, samples were prepared by dissolving the polymers in DI water at a concentration of 0.1 mg mL^{-1}, followed by adjusting the pH of the solution to pH = 7.5. Then, the polymer solutions were filtered through a 0.45 μm syringe filter, followed by drop-casting on freshly cleaved silicon wafer and dried at room temperature for 24 h in the open air, and then for 24 h under a high vacuum. The AFM experiment was carried out at ambient conditions in a semi-contact mode. For the FE-SEM study, a dried sample was coated with gold–palladium alloy (20 : 80) and micrographs were taken by the instrument at room temperature. For both AFM and FE-SEM studies, three to four images were recorded from the same slide and the size of the many assemblies was measured. Then, the average value of the many assemblies was calculated and reported as an average diameter.

Results and discussion

RAFT-SCVP of Boc-Val-HEA and VBBT

The synthesis of hyperbranched polymers *via* RAFT polymerization using divinyl cross-linkers may sometimes lead to insoluble gel formation, although this is less favourable compared to the SCVP-RAFT technique involving the AB* inimer (polymerizable chain transfer agent), which does not involve any gelation reaction.[37,38] VBBT is such an inimer that can act both as CTA due to the presence of thiocarbonylthio moiety, as well as a monomer, to form the branching unit during the

polymerization reaction due to the presence of the styryl moiety. Although the styryl group has a different reactivity compared to (meth)acrylate monomers, VBBT was chosen as the RAFT inimer for the copolymerization of acrylate monomer Boc-Val-HEA to prepare hyperbranched copolymers with variable degrees of branching and molecular weights, since trithiocarbonate CTAs are suitable for the RAFT polymerization of acrylate, methacrylate and styrenic monomers.[39] The RAFT copolymerizations of Boc-Val-HEA and VBBT were conducted in DMF as the solvent in the presence of AIBN as the radical source at 70 °C under a N$_2$ atmosphere (Scheme 1). The feed ratios of [Boc-Val-HEA]/[VBBT] were varied from 5/1 to 100/1, while keeping the molar ratios of [VBBT]/[AIBN] = 10/1 constant. The results from copolymerization reactions are summarized in Table 1. The resultant hyperbranched copolymers were characterized by ^{1}H NMR spectroscopy, where the typical resonance signals of the protons for both the Boc-Val-HEA and VBBT monomers are assigned in Fig. 1. Resonance signals from Boc-N*H*–, –O–C*H*$_2$–C*H*$_2$–O– + chiral C*H*–, and Boc group –C(C*H*$_3$)$_3$ protons appeared at 5.46–5.00, 4.46–3.76 and 1.44 ppm, respectively. The aromatic protons originating from VBBT gave a peak at 7.34–6.60 ppm. Moreover, signals due to the two types of groups connected to the terminal trithiocarbonate functionality have also been observed. The proton signal of –C*H*–S–C(=S)–, which is connected to the terminal Boc-Val-HEA unit and –C$_6$H$_4$–C*H*$_2$–S– of VBBT with pendant unreacted trithiocarbonate functionality, appeared at 4.86 and 4.56 ppm, respectively. No signal was observed in the range of 6.73–5.22 ppm due to the vinyl groups of Boc-Val-HEA and VBBT, confirming the complete elimination of unreacted monomer and inimer from the polymer matrix after purification. The copolymers were found to be soluble in most organic solvents, such as acetone, ethyl acetate, diethyl ether, chloroform, DCM, MeOH, THF, DMSO, DMF, and acetonitrile, but insoluble in water, toluene, benzene, hexanes, and petroleum ether. The hyperbranched copolymers were named accordingly: HB stands for hyperbranched polymer and the number 5, 10, 25, 50 or 100 represents the [monomer]/[CTA] ratio. Hence, for example, HB5 hyperbranched copolymer was synthesized by SCVP-RAFT with a [Boc-Val-HEA]/[CTA] ratio of 5/1. Boc-deprotected polymers will be represented as DHB, where D stands for Boc deprotection.

With the variation of the feed compositions of [Boc-Val-HEA]/[VBBT] from 5/1 to 100/1, the $M_{n,GPC}$ of hyperbranched copolymers varied from 8100 to 31 000 g mol^{-1} with a relatively low PDI in the range of 1.24–1.89 (Table 1). However, the $M_{n,GPC}$ values are very high compared to the theoretical molecular weight ($M_{n,theo}$), calculated considering the formula of the linear RAFT polymerization ($M_{n,theo}$ = (([Boc-Val-HEA]/[VBBT] × molecular weight (MW) of Boc-Val-HEA × conversion) + (MW of VBBT)), which is the typical characteristic of hyperbranched copolymerization reactions.[40,41] This could be due to the different synthetic mechanisms of the RAFT homopolymerization and the SCVP-RAFT technique. Note that actual $M_{n,GPC}$ values of hyperbranched polymers are expected to be higher than the observed $M_{n,GPC}$ values obtained from the
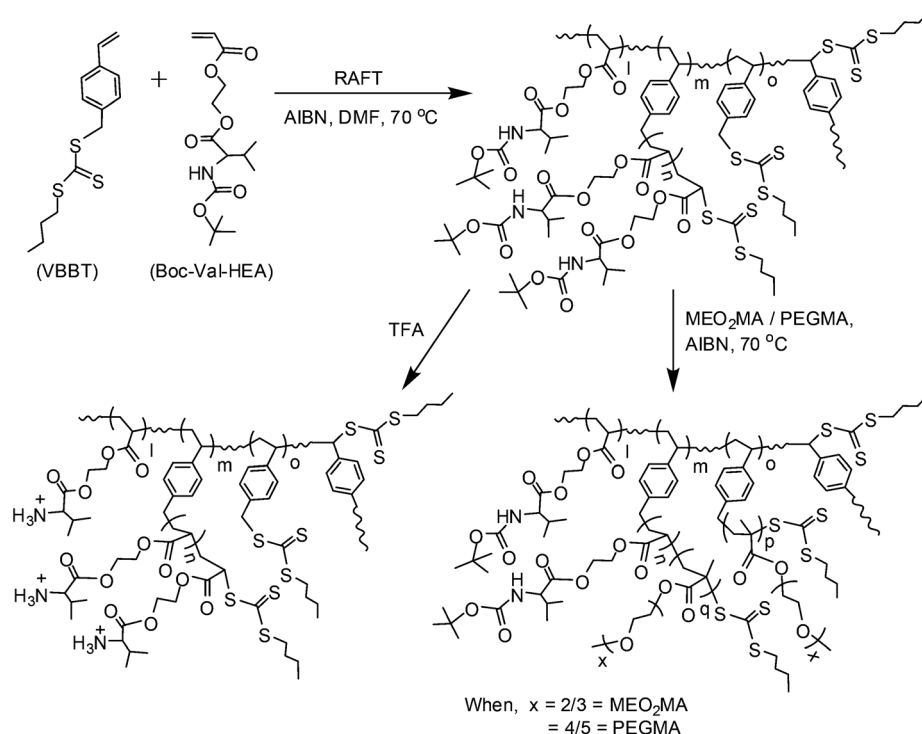
Scheme 1 Synthesis of hyperbranched copolymers P(Boc-Val-HEA-*co*-VBBT) and the corresponding star polymers by RAFT polymerization, followed by deprotection of the Boc groups from hyperbranched polymers.

Table 1 Results of RAFT-SCVP copolymerization of Boc-Val-HEA with VBBT in DMF at 70 °C under various reaction conditions[a]

Entry	[M]/[CTA]/[AIBN]	Time (h)	Conv.[b] (%)	$M_{n,theo}$[c] (g mol^{-1})	$M_{n,GPC}$[d] (g mol^{-1})	PDI[d]	RB(th)[e]	DB[f]	RB (NMR)[g]
1	5/1/0.1	12	86.4	1640	8100	1.24	5.32	0.1897	5.27
2	10/1/0.1	12	83.1	2900	9700	1.20	9.31	0.1125	8.89
3	10/1/0.1	24	98.0	3370	10 500	1.20	10.80	0.1383	7.23
4	25/1/0.1	12	87.9	7210	9800	1.32	22.98	0.0881	11.35
5	25/1/0.1	24	98.2	8020	10 800	1.27	25.55	0.0440	22.72
6	50/1/0.1	12	80.2	12 930	13 500	1.40	41.10	0.0580	17.24
7	100/1/0.1	12	93.1	29 640	31 000	1.89	94.10	0.0232	43.10
8	10/1/0.1	24	98.9	3400	16 500	1.41	10.89	0.1287	7.77
9	10/1/0.1	18	71.8	2550	16 200	1.45	8.18	0.1725	5.78
10	5/1/0.1	4.30	92.3	1740	10 700	1.31	5.62	0.2181	4.59
11	10/1/0.1	4.30	86.4	3000	12 000	1.34	9.64	0.1808	5.53
12	25/1/0.1	4.30	88.1	7230	14 700	1.48	23.03	0.0923	10.83

[a] Entries 1–7: [Boc-Val-HEA] = 1.0 mol L^{-1}; entries 8 and 10–12: [Boc-Val-HEA] = 3 mol L^{-1}; entry 9: [Boc-Val-HEA] = 5 mol L^{-1}. [b] Calculated by ^{1}H NMR spectroscopy. [c] The theoretical molecular weight ($M_{n,theo}$) = ([Boc-Val-HEA]/[VBBT] × molecular weight (MW) of Boc-Val-HEA × conversion) + (MW of VBBT). [d] Measured by GPC in THF. [e] Theoretical repeat unit per branch (RB), calculated from the equation RB(th) = [Boc-Val-HEA] × conversion of Boc-Val-HEA + 1. [f] Determined by ^{1}H NMR spectroscopy, DB = $2(I_{7.34-6.60}/4 - I_{4.56}/2)/(I_{7.34-6.60}/4 + I_{1.44}/9 - 1)$, where I stands for the integration area of various chemical shift of protons. [g] RB = 1/DB.

conventional GPC characterization, which is calibrated with linear PMMA homopolymer standards. Hyperbranched polymers have different hydrodynamic volumes compared to their linear analogues due to their compact structure and high segment density. Unimodal GPC-RI traces (Fig. 2) with relatively narrow PDI (1.31) for hyperbranched copolymers were obtained from the molar ratios of 5/1 and 10/1. Whereas higher ratios such 25/1, 50/1 and 100/1 gave bimodal distributions in the GPC-RI traces. This observation can be explained by the different rate of the copolymerization reaction

due to the different molar proportions of Boc-Val-HEA with respect to the VBBT. Initially, VBBT may be consumed as CTA, and then it forms a linear homopolymer of Boc-Val-HEA with terminal trithiocarbonate functionality. However, in the case of lower molar proportions (5/1 and 10/1), the rate of the reversible addition–fragmentation slowed down due to the limited monomer availability; hence, some trithiocarbonate remained unreacted in the resultant branched copolymer, P(Boc-Val-HEA-*co*-VBBT). Moreover, more numbers of VBBT participated as co-monomer in the co-polymerization reaction,
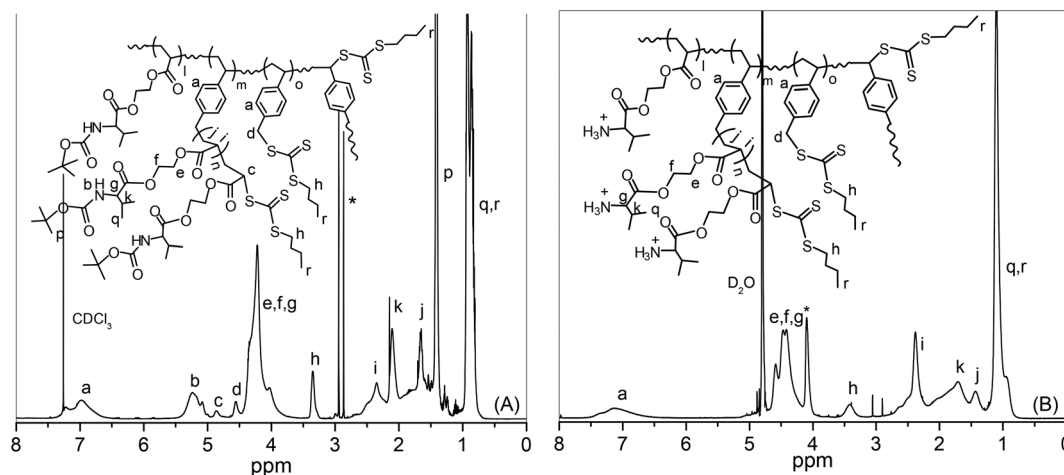
Fig. 1 ^{1}H NMR spectra of (A) P(Boc-Val-HEA-co-VBBT) hyperbranched copolymer (synthesized by RAFT-SCVP at [Boc-Val-HEA]/[VBBT] = 5/1) in CDCl$_3$ and (B) corresponding Boc deprotected polymer in D$_2$O.

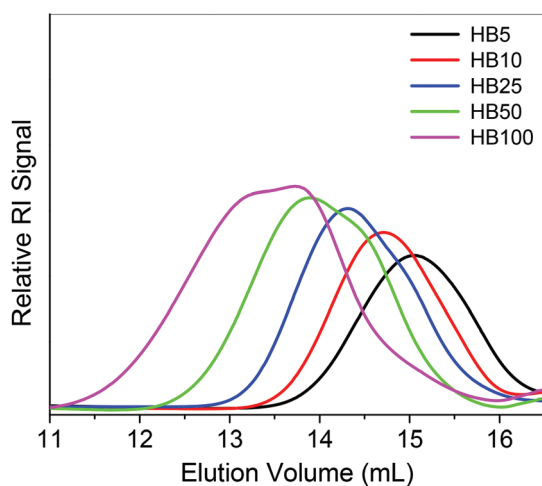**Fig. 2** GPC-RI traces of P(Boc-Val-HEA-co-VBBT) hyperbranched copolymers synthesized by SCVP-RAFT with different feed ratios of [Boc-Val-HEA]/[VBBT].

leading to the formation of a branched copolymer with unimodal GPC-RI traces. As the [Boc-Val-HEA]/[VBBT] ratio increased, the molar concentration of Boc-Val-HEA increased in the polymerization system compared to VBBT; hence, the rate of polymerization of Boc-Val-HEA was high, resulting into the formation of propagating linear homopolymers. Moreover, the styryl group of VBBT (containing propagating radical) participated in the copolymerization reaction, leading to the formation of branched polymers. Since the styryl group of VBBT has a different reactivity with respect to the acrylate group of Boc-Val-HEA monomer, branched polymers are formed with the bimodal distribution in the case of the monomer to inimer ratio being greater than 10/1.

The influence of monomer concentration during the SCVP-RAFT copolymerization was studied by varying the Boc-Val-HEA concentration from 1.0 (entry 3 in Table 1) to 3.0

(entry 8 in Table 1) to 5.0 mol L^{-1} (entry 9 in Table 1), keeping constant ratios of [Boc-Val-HEA]/[VBBT]/[AIBN] = 10/1/0.1. Table 1 shows that with the increase of monomer concentration, both the molecular weight and PDI increases. The rate of the RAFT polymerization reaction slows down with dilution of the monomer concentration and hence the rate of propagation decreases, leading to the formation of propagating radicals with lower molecular weight. Since the movement (diffusion) of the propagating radicals with low molecular weight is free, CTA can easily interact with radicals, resulting in branched polymers with narrow PDI. Therefore, branched P(Boc-Val-HEA-co-VBBT) copolymers with low molecular weight and PDI can be achieved by slowing down the rate of the RAFT polymerization reaction.

Degree of branching analysis

The degree of branching is an important parameter that describes the fraction of branching units present within the macromolecules with branched structures. For the SCVP-RAFT, DB was calculated by ^{1}H NMR spectroscopy using the equation DB = 2(number of branched units)/(total number of units − 1).[42,43] The number of branching unit was calculated from ($I_{7.34-6.60}/4 - I_{4.56}/2$), whereas ($I_{7.34-6.60}/4 + I_{1.44}/9$) represented the total number of units present in the P(Boc-Val-HEA-co-VBBT) branched copolymers. The P(Boc-Val-HEA-co-VBBT) with the ratio of [Boc-Val-HEA]/[VBBT] = 5 led to the highest DB of 0.1897, and average repeat unit of branch (RB), ~5.27, whereas the lowest DB was observed for the ratio of 100/1 with a DB of 0.0232 and a corresponding average RB of 43.1. Table 1 lists the DB of branched polymers decreasing with the increase of [Boc-Val-HEA]/[VBBT] ratios from 5/1 to 100/1. The branching points are introduced into the polymer chain due to the participation of both the styryl unit and the trithiocarbonate functionality in the VBBT. With the increasing ratio of [Boc-Val-HEA]/[VBBT] from 5/1 to 100/1, the population of VBBT decreased in the polymerization reaction mixture; hence, the number of branching points decreased.

Therefore, DB and RB could be tuned by varying the reaction stoichiometry.

Kinetics of SCVP-RAFT mediated copolymerization

In the next stage, the copolymerization kinetics was investigated with [Boc-Val-HEA]/[VBBT]/[AIBN] = 5/1/0.1, 10/1/0.1 and 25/1/0.1 at 70 °C in DMF to study the time dependent change of the M_n, PDI and DB of the resultant copolymers during the RAFT-SCVP copolymerization of Boc-Val-HEA with VBBT. At regular intervals, approximately 0.1 mL of the polymerization reaction mixture was analyzed by ^{1}H NMR spectroscopy and GPC to monitor the monomer conversion, DB, RB and M_n. In the ^{1}H NMR spectra of the reaction mixtures, the intensity of the resonance signals of the acryloyl group from Boc-Val-HEA at 6.16–6.08 (HC=CH$_2$, 1H, m), 6.46–6.39, and 5.88–5.83 ppm (HC=CH_2, 2H, d) become weaker as the reaction proceeds. However, the styrenic double bond, which resonates at 6.73–6.65 (CH_2=CH, 1H, m), 5.75–5.70 and 5.26–5.22 ppm (CH_2=CH, 2H, d), disappeared after 1 h, indicating that all the styryl moieties participated in the polymerization reaction. The conversion of Boc-Val-HEA was determined by comparing the peak intensities of CH$_2$=CH proton at 6.16–6.08 ppm at zero time and at time t to the DMF peak intensity at 8.02 ppm. The rate of the monomer conversion increased with the increase of the [Boc-Val-HEA]/[VBBT] ratio from 5/1 to 25/1 as expected due to the decrease of the CTA concentration (Fig. 3A). 41.6%,

58.5%, and 67.5% conversions were achieved within 1 h for the [Boc-Val-HEA]/[VBBT] ratios of 5/1, 10/1, and 25/1, respectively. However, almost 90% conversion was achieved within 3 h, and then the polymerization reaction slowed down, and it took 12 h to reach close to 100% conversion. This phenomenon could be attributed to the fact that RAFT-SCVP copolymerization of Boc-Val-HEA with VBBT is expected to proceed by the rapid addition of the initiator-induced oligomer radicals to the trithiocarbonate functionality of VBBT, followed by fragmentation of the RAFT adduct radical with styryl functionality (macro-CTA), which starts the copolymerization reaction between Boc-Val-HEA and VBBT to yield the polymer chains with pendant trithiocarbonate functionality and terminal styryl groups. The pendant trithiocarbonate functionality could participate in the RAFT polymerization with the remaining monomer, Boc-Val-HEA, whereas terminal styryl groups were integrated into the other chain, leading to the formation of branched polymers. Therefore, RAFT copolymerization reactions occurred with chain growth, as well as by step growth, characteristic with broader PDI and high M_n compared to the theoretical molecular weight assuming VBBT as normal CTA.

The GPC-RI traces of polymers moved towards the lower elution volume with the increasing monomer conversion (Fig. 3C, Fig. S7A and S7B†). The dependence of M_n of the resulting branched copolymers from the conversion of Boc-Val-HEA is shown in Fig. 3B. At lower monomer conversions,
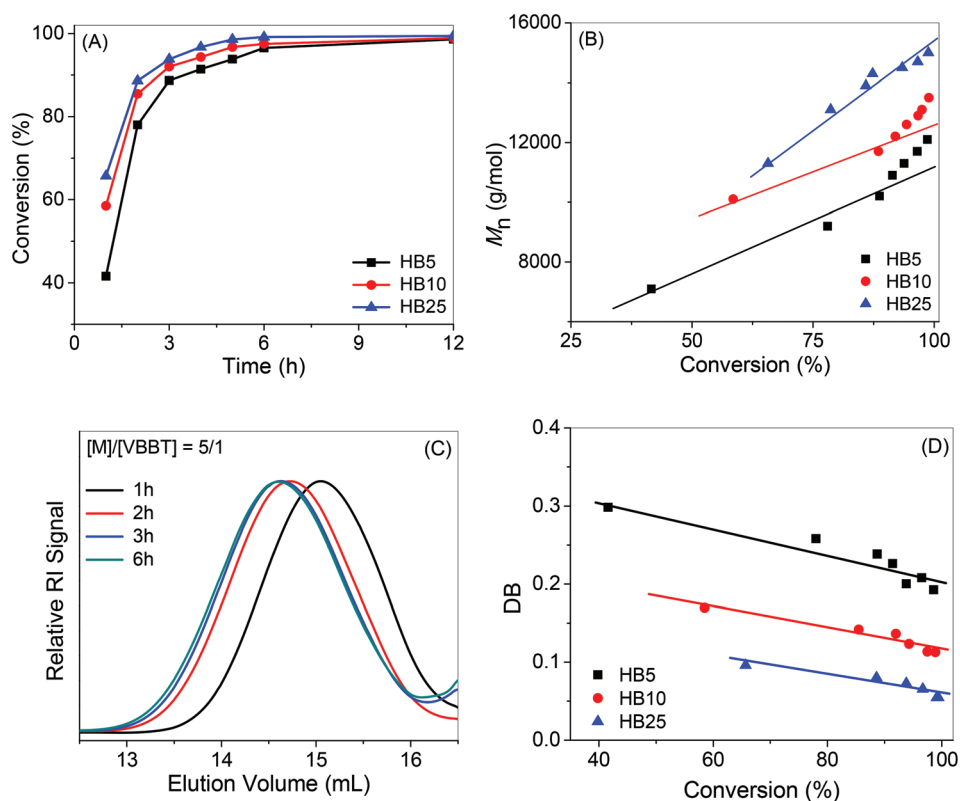

Fig. 3 (A) Conversion of Boc-Val-HEA as a function of time, and (B) evolution of M_n with the monomer conversion for the SCVP-RAFT of Boc-Val-HEA with VBBT at different feed ratios of [Boc-Val-HEA]/[VBBT]. GPC-RI traces as function of time at [Boc-Val-HEA]/[VBBT] = 5/1 (C), and DB as a function of conversions (D).

Table 2 Aqueous solution properties of linear P(Boc-Val-HEA) and hyperbranched copolymers

Polymer	[M]/[CTA]/[AIBN][a]	Time (min)	Conv.[b] (%)	T_g[c] (°C)	Deprotected Polymers	Transition pH[d]	ξ[e] (mV)
HB5	5/1/0.1	270	92.3	35.2	DHB5	6.8	25.3
HB10	10/1/0.1	270	95.8	37.2	DHB10	7.0	25.1
HB25	25/1/0.1	270	97.2	39.0	DHB25	7.3	23.3
HB50	50/1/0.1	270	83.1	39.3	DHB50	7.4	20.4
HB100	100/1/0.1	270	86.6	40.1	DHB100	7.5	16.5
P(Boc-Val-HEA)	50/1/0.1	300	68.1	37.6	P(H$_3$N$^+$-Val-HEA)	7.5	15.3

[a] Polymerization conditions: [Monomer] = 3 mol L^{-1}, in DMF at 70 °C. VBBT was used as the inimer-CTA for hyperbranched polymer synthesis and CDP was used for the synthesis of linear homopolymer. [b] Determined by gravimetric analysis. [c] Obtained from DSC studies. [d] Determined by UV-Vis spectroscopy. [e] Measured by DLS at pH = 7.

the M_n of the polymers increased linearly with the conversion, as the process followed the living polymerization of Boc-Val-HEA, where VBBT acts as a normal CTA. However, deviations from the linear relationship are observed at higher conversions with a sharper increase of M_n due to the linking reaction between the double bond of the pre-formed macromolecules and the active centre of the propagating radicals, which is the common characteristic of the SCVP copolymerization technique.[44,45]

The DB of hyperbranched polymers prepared from the SCVP-RAFT copolymerization reaction mainly depends on the [monomer]/[inimer] ratio, the reactivity ratio of the co-monomers and the ratio of the rate constants of the homopolymerization reaction.[46] It can be observed in Fig. 3D that DB decreases with the increase in the [monomer]/[inimer] ratio from 5/1 to 25/1, in a linear fashion with the monomer conversion. The branching points are introduced into the system by both the styryl unit and from the trithiocarbonate functionality during the SCVP-RAFT copolymerization. However, the concentration of the styryl unit decreases with time and the maximum DB is observed after 1 h. All the VBBT are consumed within this time and the DB values decrease linearly as the reaction proceeds due to the participation of the remaining monomers in the RAFT copolymerization and/or due to the additions to the trithiocarbonate functionality to increase the chain length and to increase the repeat unit per branch. Wei et al. reported similar decreases in DB for the RAFT polymerization of galactose-based saccharide monomers in the presence of 2-(methacryloyloxy)ethyl 4-cyano-4-(phenylcarbonothioylthio) pentanoate and 2-(3-(benzylthiocarbonothioylthio) propanoyloxy)ethyl acrylate RAFT inimers.[47]

Since the thermal properties of hyperbranched and star polymers usually differ from their linear analogue due to their various degrees of branching,[48] the thermal characteristics of the branched copolymers P(Boc-Val-HEA-co-VBBT) and linear P(Boc-Val-HEA) homopolymer were investigated by DSC (Fig. S8†). In the DSC thermogram of the branched copolymers, a single T_g was observed ranging from 35.2 °C to 40.1 °C, indicating a good compatibility between Boc-Val-HEA and VBBT units in the copolymers. The T_g values are reported in Table 2, which shows the increment of T_g values with the increased chain length due to the restricted chain mobility. With increasing DB, the free volume of branched polymers

increased due to the increased number of chain ends, which decreased the T_g value.

Star polymer synthesis via RAFT polymerization using hyperbranched core

The synthesis of star polymers from hyperbranched polymers is a facile and straightforward approach compared to other methods, such as the arm-first,[49,50] core-first[51,52] and combination of both.[53,54] In the arm-first method, prefabricated arms were synthesized via controlled/living polymerizations, followed by reaction with the multifunctional core to produce star polymers. The major drawback of this process is that the number of arms is uncertain due to efficiency of the coupling reactions; moreover, sometimes purification of the targeted star polymer can be tedious. In the core-first method, the multifunctional core is generally prepared via a multi-step organic synthesis, followed by the fabrication of arms from the core. The disadvantage of this process lies in the multi-step organic synthesis followed by rigorous purification. These disadvantages could be tackled with the synthesis of star polymers from a hyperbranched core obtained via a one-step SCVP-RAFT polymerization reaction, and then the number of arms of stars could be tuned by controlling the chain end functionality in the hyperbranched core with variation of the [monomer]/[inimer] ratio.[55] In this study, P(Boc-Val-HEA-co-VBBT) hyperbranched copolymers with multiple trithiocarbonate CTA functionality could be used as the macro-CTA for the synthesis of star-shaped polymers (Scheme 2). The star polymers P(HB5-star-PEGMA), P(HB10-star-MEO$_2$MA) and P(HB25-star-MEO$_2$MA) were synthesized by RAFT polymerization using HB5, HB10 and HB25 as macro-CTAs with [monomer]/[P(Boc-Val-HEA-co-VBBT)-macro CTA]/[AIBN] = 150/1/0.1 for P(HB5-star-MEO$_2$MA) and 100/1/0.1 for P(HB10-star-MEO$_2$MA) and P(HB25-star-MEO$_2$MA) in DMF at 70 °C, respectively. The HB5 (78.0% conversion, $M_{n,GPC}$ = 8200 g mol^{-1}, PDI = 1.38), HB10 (85.5% conversion, $M_{n,GPC}$ = 10 700 g mol^{-1}, PDI = 1.36) and HB25 (88.6% conversion, $M_{n,GPC}$ = 13 100 g mol^{-1}, PDI = 1.43) were prepared via SCVP-RAFT polymerization in DMF at 70 °C for 2 h with feed ratios of [Boc-Val-HEA]/[VBBT] = 5/1, 10/1 and 25/1, respectively.

Details of the synthesis of star polymers are summarized in Table 3. The GPC-RI traces of the resultant star polymers are
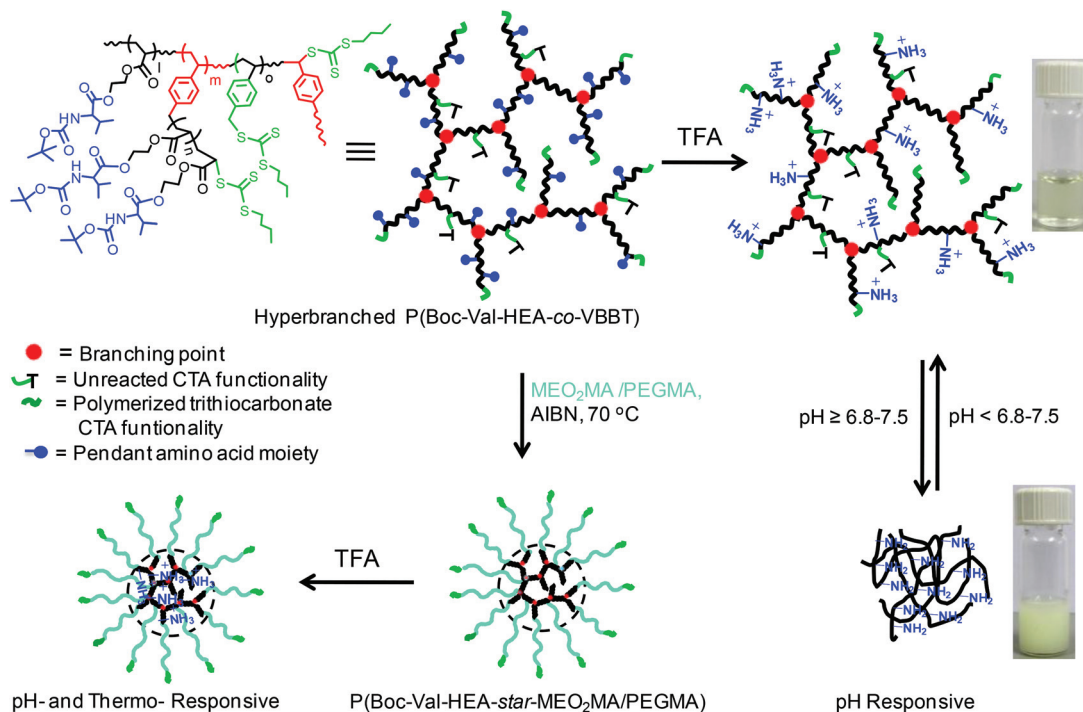
Scheme 2 Schematic representation of synthesis of pH responsive hyperbranched polymers and their respective star polymers with hyperbranched core *via* successive RAFT process.

Table 3 Results from star polymer synthesis *via* RAFT polymerization using hyperbranched core[a]

Polymer	Monomer	[M]/[Macro-CTA]/[AIBN]	Time (min)	Conv.[b] (%)	$M_{n,theo}$[c] (g mol^{-1})	$M_{n,GPC}$[d] (g mol^{-1})	PDI[d]
P(HB5-*star*-PEGMA)	PEGMA	150/1/0.1	230	53.2	32 140	25 300	1.54
P(HB10-*star*-MEO$_2$MA)	MeO$_2$MA	100/1/0.1	340	65.8	23 080	14 300	1.59
P(HB25-*star*-MEO$_2$MA)	MeO$_2$MA	100/1/0.1	320	70.4	26 350	25 700	2.84

[a] Polymerization conditions: in DMF solvent at 70 °C with [Monomer (M)] = 1 mol L^{-1}. [b] Determined by gravimetric analysis. [c] $M_{n,theo}$ = (M_n of macro-CTA + ([Monomer]/[macro-CTA] × molecular weight of monomer × conversion)). [d] Measured by GPC in THF.
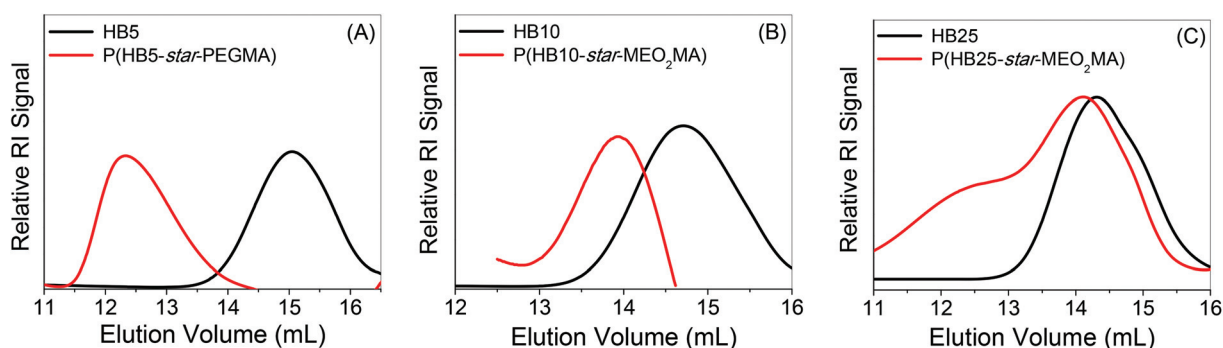

Fig. 4 GPC RI traces of the (A) HB5 macro-CTA and P(HB5-*star*-PEGMA), (B) HB10 macro-CTA and P(HB10-*star*-MEO$_2$MA), and (C) HB25 macro-CTA and P(HB25-*star*-MEO$_2$MA).

moved to the lower elution volume with an almost unimodal distribution for P(HB5-*star*-PEGMA) and P(HB10-*star*-MEO$_2$MA), suggesting no bimolecular termination or star–star coupling reactions occur during the polymerization (Fig. 4). However, a bimodal GPC-RI trace has been observed for the

P(HB25-*star*-MEO$_2$MA) star polymers with broader PDI may be due to the loss of CTA functionality or star–star coupling reaction. The $M_{n,GPC}$ for P(HB5-*star*-PEGMA), P(HB10-*star*-MEO$_2$MA) and P(HB25-*star*-MEO$_2$MA) polymers are much lower than the $M_{n,theo}$ values calculated from the monomer
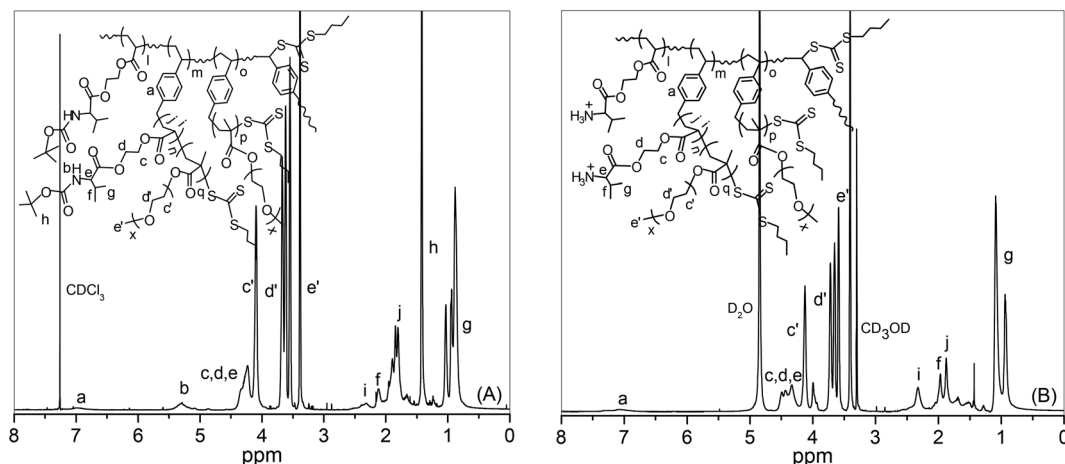
Fig. 5 ^{1}H NMR spectra of (A) P(HB10-*star*-MEO$_2$MA) star polymer in CDCl$_3$ and (B) Boc de-protected P(HB10-*star*-MEO$_2$MA) star polymer in CD$_3$OD.

conversion (Table 3) due to the compact nature of the star polymers.[56] The typical ^{1}H NMR spectra (Fig. 5A) for the star polymers show characteristic signals for both the Boc-Val-HEA and PEGMA/MEO$_2$MA units.

Aqueous solution properties of the hyperbranched polymers

First, removal of the Boc groups of the pendant amino acid moieties in the linear P(Boc-Val-HEA), hyperbranched copolymers, and the corresponding star polymers were accomplished in the presence of TFA at room temperature to obtain polymers with primary ammonium (–NH$_3^+$) salts (Scheme 2). After the Boc group deprotection, all the polymers became soluble in aqueous medium. The evidence for the successful Boc deprotection was demonstrated by the ^{1}H NMR spectroscopy, where the resonance signal for the *tert*-butyl group at 1.44 ppm completely disappeared in the de-protected hyperbranched polymer, P(H$_3$N$^+$-Val-HEA-*co*-VBBT) (Fig. 1B), and in the respective star polymer (Fig. 5B). Moreover, additional evidence of the Boc deprotection was established by the FT-IR study, where secondary N–H bending at 1501 cm^{-1} in the Boc-protected hyperbranched polymer (Fig. S9†) disappeared after the Boc group deprotection, and a small peak then appeared at 1539 cm^{-1} in the de-protected hyperbranched polymers due to the formation of –NH$_3^+$. Similar results were noticed in the FT-IR spectra of Boc-protected and corresponding de-protected star polymers, except for variations in the intensities of the different peaks.

Branched polymers synthesized *via* RAFT-SCVP contain multiple hydrophobic chain termini, which might have a significant effect on the solution properties of branched polymers.[57] Furthermore, deprotected polymers are expected to show pH-responsive properties due to the protonation/deprotonation ability of the primary amine groups present in the pendant amino acid moiety.[58] Hence, the pH-induced solution behaviour of hyperbranched copolymers was investigated by UV-Vis spectroscopy at 500 nm by analyzing their aqueous solution (2 mg mL^{-1}) as a function of pH. Initially, the pH of

the solution was adjusted to 3.0, and subsequently the pH was incrementally increased approximately in an interval of 0.5 units, followed by the measurement of the % transmittance (%T) at 500 nm. A reduction of 50% T of the polymer solution was considered as the transition pH (Fig. 6). The transition pH for the deprotected homopolymer, P(H$_3$N$^+$-Val-HEA), was found to be 7.5, whereas the transition pH for the hyperbranched copolymers increased from 6.8 for DHB5 to 7.5 for DHB100 with the increase of feed ratio [Boc-Val-HEA]/[VBBT] from 5/1 to 100/1, and the results are summarized in Table 2. Since, the CTA-derived end group has a considerable effect on the overall aqueous solution property of the polymers;[23] thus, the observed phenomenon could be caused by the fact that the number of hydrophobic VBBT moieties increased with the increase of DB, which increased the overall hydrophobicity of the branched polymer. Moreover, the overall charge density due to the protonated pendant amino acid units of the branched polymers increased with the increase of DB. Thus, the apparent pK_b value (corresponding to 50% ionization) of
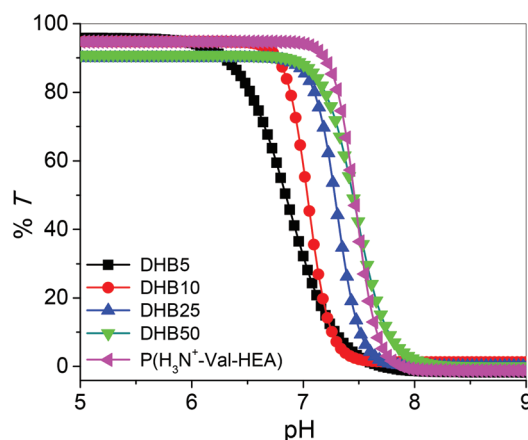

Fig. 6 Plot of transmittance at 500 nm *versus* pH for the aqueous solutions of Boc-deprotected homopolymer and hyperbranched copolymers (2 mg mL^{-1}) at 25 °C.

the branched polymers increased with the increasing DB.[59] Sumerlin and co-workers reported that the lower critical solution temperature (LCST) of N-isopropyl acrylamide-based hyperbranched polymers significantly reduced with the increased degree of branching as compared to the linear analogue due to the incorporation of a higher number of hydrophobic end group functionalities.[23] Luzon et al. also reported a RAFT-based hyperbranched system where the LCST of hyperbranched copoly(oligoethylene glycol)s decreased about 5–10 °C compared to its linear chains.[60]

Deprotected homopolymer and hyperbranched copolymers are also expected to show positive surface charges due to the presence of primary amine functionality in the pendant amino acid unit.[61] This was verified by measuring the zeta potential (ξ) of aqueous solutions (1 mg mL^{-1}) of various deprotected polymers at pH 7.0, and results are listed in Table 2. The net positive ξ indicates the presence of the primary amine functionality in the homo- and hyper-branched co-polymers. Since the charge density of hyperbranched polymers is proportional to the DB, ξ increased with the increase of DB from 16.5 for DHB100 to 25.2 for DHB5. Note that the ξ values of DHB100 and linear homopolymer are the same due to the very little DB in DHB100. Since branched PEIs are very efficient in gene delivery,[62] the present pH-responsive cationic hyperbranched polymers are also expected to be promising materials for gene and siRNA delivery applications.

Aqueous solution properties and the self-assembly of star polymers

Boc-deprotected star polymers are composed of a pH-responsive hydrophilic core with pendant primary amine units and hydrophilic thermoresponsive multi-arms composed of PEGMA/MEO$_2$MA. To study their solution properties, the numbers of arms of the stars and their core topologies were varied. The polymers were dissolved in water (1 mg mL^{-1}) and the size distributions of the star polymers were studied by DLS at different pH and temperature (Fig. 7 and S10†). Below the

Fig. 7 Size distributions detected by DLS with the solution of 1 mg mL^{-1} at different pH and temperature for P(DHB10-star-MEO$_2$MA) (blue) and P(DHB25-star-MEO$_2$MA) (red).

phase transition pH (at pH = 4.0), the average hydrodynamic diameters (D_h) were found to be 4 ± 1, 4 ± 1 and 5 ± 1 nm for the P(DHB5-star-PEGMA), P(DHB10-star-MEO$_2$MA), and P(DHB25-star-MEO$_2$MA), respectively, corresponding to the unimers in solution. Above the phase transition pH (at pH = 7.5), D_h values were found to be 21 ± 2 nm for P(DHB5-star-PEGMA), 179 ± 4 nm for P(DHB10-star-MEO$_2$MA) and 299 ± 4 nm for P(DHB25-star-MEO$_2$MA) at 16 °C, indicating the pH-induced self-assembly of star polymers above their transition pH (Table 4). In the case of P(DHB5-star-PEGMA), the D_h value is low, which is a common characteristic of star polymers due to their spherical and compact structure, indicating the uni-micellar aggregation, whereas high D_h values of P(DHB10-star-MEO$_2$MA) and P(DHB25-star-MEO$_2$MA) (at pH = 7.5 and 16 °C) indicate the formation of multi-micellar aggregation (MMA).[63] After the Boc group expulsion, star polymers with pendant primary amine units in the core should show a cationic character (net positive ξ) at pH = 7 (Table 4). However, the ξ values of the star polymers are quite low compared to their corresponding hyperbranched copolymer cores, possibly due to the steric shielding effect offered by PEGMA and MEO$_2$MA chains.[64]

More accurate evidence for the aggregation of star polymers with hyperbranched cores was obtained from SEM and AFM imaging techniques. Fig. 8 shows the SEM micrograph of P(DHB10-star-MEO$_2$MA) and P(DHB25-star-MEO$_2$MA) star polymers, where samples were prepared by drop-casting of aqueous solutions of polymers (0.1 mg mL^{-1}) at pH = 7.5 and at a particular temperature (16 or 26 °C). The observed diameters of the self-assembled star polymers at different pHs and temperatures are listed in Table 4, and are somewhat less than the DLS values, which is quite common as the size of hydrated aggregates is higher than the dried one.[65] Due to the spherical size and compact nature of the hyperbranched core, star polymers are expected to show a small hydrodynamic volume with a uni-micellar self-assembled aggregation. However, very large sizes with 150 and 276 nm diameters were obtained in SEM images for P(DHB10-star-MEO$_2$MA) and P(DHB25-star-MEO$_2$MA) star polymers, respectively, probably due to the formation of MMA with amino acid-based hyperbranched cores at pH = 7.5 and many hydrophilic MEO$_2$MA arms. Below the transition pH, star polymers remained as unimers in solution that self-assembled to form uni-micellar aggregates, which further underwent MMA above the transition pH of the hyperbranched core. Scheme 3 shows the self-assembly mechanism of MMA.[66]

The LCST of P(DHB10-star-MEO$_2$MA) and P(DHB25-star-MEO$_2$MA) was found to be 22.8 and 22.5 °C, respectively, and were determined by UV-Vis spectroscopy (see ESI and Fig. S11†). These LCST values are a little low compared to the actual LCST of PMEO$_2$MA (LCST = 26 °C).[67] Above the LCST of these star polymers, the MMAs are fused together to a larger aggregate with a diameter of ~500 nm as determined from the SEM images in Fig. 8B and 8D. Further evidence of the aggregation of the star polymers is obtained from the AFM (Fig. S12 and S13†) analysis, and here too the sizes are in good agreement with the DLS and SEM measurements.
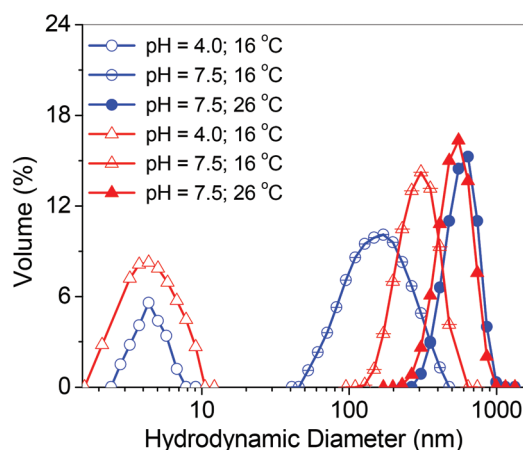
Table 4 Aqueous solution properties and self-assembly of deprotected star polymers

Polymer	ξ^a (mV) at pH = 7.0	Size^a (nm) (Dispersity)			SEM^b (nm)		AFM^c (nm)	
		pH = 4.0, 16 °C	pH = 7.5, 16 °C	pH = 7.5, 26 °C	pH = 7.5, 16 °C	pH = 7.5, 26 °C	pH = 7.5, 16 °C	pH = 7.5, 26 °C
P(DHB5-star-PEGMA)	1.4	4 ± 1 (0.218)	21 ± 2 (0.205)	—	22	—	22	—
P(DHB10-star-MEO$_2$MA)	3.7	4 ± 1 (0.262)	179 ± 4 (0.378)	586 (0.204)	150	456	155	450
P(DHB25-star-MEO$_2$MA)	4.2	5 ± 1 (0.532)	299 ± 4 (0.262)	600 (0.342)	276	487	254	520

^{a} Determined by DLS. ^{b} Obtained from SEM study. ^{c} Determined from AFM measurement.
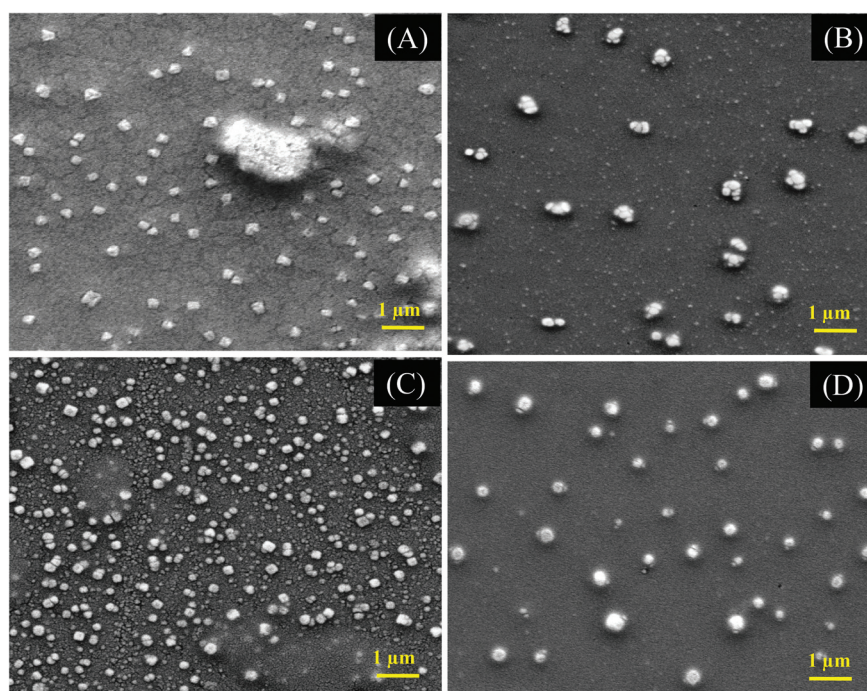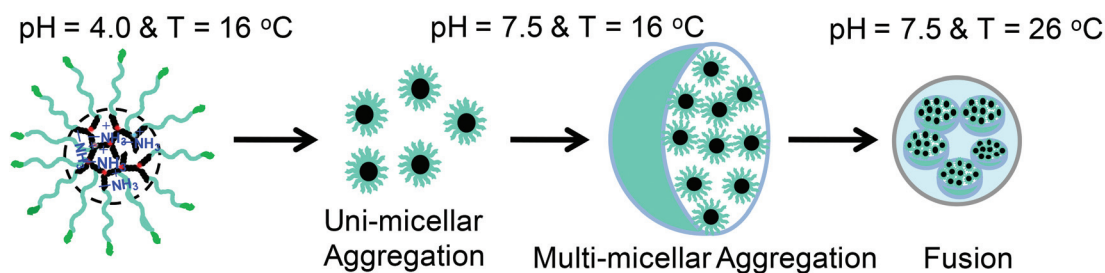

Fig. 8 SEM micrograph of P(DHB10-star-MEO$_2$MA) at (A) pH = 7.5 and 16 °C, and (B) pH = 7.5 and 26 °C. SEM images of P(DHB25-star-MEO$_2$MA) at (C) pH = 7.5 and 16 °C, and (D) pH = 7.5 and 26 °C. Samples were prepared from 0.1 mg mL^{-1} aqueous polymer solutions.

Scheme 3 Schematic representation of the self-assembly of the P(DHB10-star-MEO$_2$MA) and P(DHB25-star-MEO$_2$MA) star polymers with a pH-responsive amino acid-based hyperbranched core (black) and hydrophilic thermoresponsive multi-arms MEO$_2$MA (green) at different pH and temperature (T).

Conclusions

In conclusion, we have demonstrated that the SCVP-RAFT copolymerization of Boc-Val-HEA and VBBT can successfully produce amino acid-based hyperbranched and star polymers.

It has been observed that the molecular weight, DB, repeat unit per branch and the chain end functionalities of hyperbranched copolymers can be altered with the variation of the co-monomer (Boc-Val-HEA and VBBT) feed compositions, the concentration of Boc-Val-HEA monomer in the polymerization

mixture and by the polymerization time. Polymerization kinetics studies with the varied [Boc-Val-HEA]/[VBBT] ratios reveal that the molecular weight of hyperbranched copolymers increase, while DB decreases linearly with the conversion. Furthermore, hyperbranched copolymers with variable DB could be employed as a macro-CTA for the synthesis of star polymers with a hyperbranched core and a varied number of arms and arm length *via* successive RAFT polymerization reactions. The expulsion of Boc groups from the protected amino acid moieties in the side chain of hyperbranched polymers afford water soluble pH-responsive hyperbranched polymers with cationic surface charges. Since the charge density of hyperbranched polymers is proportional to the DB, ξ increased with the increasing DB and the hydrophilic to hydrophobic pH transition can be tuned between 6.8 and 7.5 by altering the feed ratios of [Boc-Val-HEA]/[VBBT] during the polymerization, which will give different amounts of hydrophobic CTA functionality at the chain ends. Boc-deprotected DHB-*star*-MEO$_2$MA/PEGMA star polymers with pH-responsive core and thermoresponsive arms showed a self-assembled aggregation above the transition pH = 7.5 to a multi-micellar aggregation, which further fused together to form large aggregates above their LCST. These amino acid-based architectures with pH-responsive properties and positive ξ values are anticipated to be biocompatible due to the presence of amino acid pendants and could be explored for use as alternative and efficient gene delivery devices.

Acknowledgements

Notes and references

1 R. M. England and S. Rimmer, *Polym. Chem.*, 2010, **1**, 1533–1544.

2 Y. Shen, M. Kuang, Z. Shen, J. Nieberle, H. Duan and H. Frey, *Angew. Chem., Int. Ed.*, 2008, **47**, 2227–2230.

3 G. L. Drisko, L. Cao, M. C. Kimling, S. Harrisson, V. Luca and R. A. Caruso, *ACS Appl. Mater. Interfaces*, 2009, **1**, 2893–2901.

4 J. Chen, C. Wu and D. Oupický, *Biomacromolecules*, 2009, **10**, 2921–2927.

5 T. C. Stover, Y. S. Kim, T. L. Lowe and M. Kester, *Biomaterials*, 2008, **29**, 359–369.

6 A. B. Arote, E.-S. Lee, H.-L. Jiang, Y.-K. Kim, Y.-J. Choi, M.-H. Cho and C.-S. Cho, *Bioconjugate Chem.*, 2009, **20**, 2231–2241.

7 R. Spindler and J. M. J. Fréchet, *Macromolecules*, 1993, **26**, 4809–4813.

8 Z. Xue, A. D. Finke and J. S. Moore, *Macromolecules*, 2010, **43**, 9277–9282.

9 Y. Li and S. P. Armes, *Macromolecules*, 2005, **38**, 8155–8162.

10 F. Isaure, P. A. G. Cormack and D. C. Sherrington, *Macromolecules*, 2004, **37**, 2096–2105.

11 P. F. W. Simon, A. H. E. Müller and T. Pakula, *Macromolecules*, 2001, **34**, 1677–1684.

12 Y. Tao, J. He, Z. Wang, J. Pan, H. Jiang, S. Chen and Y. Yang, *Macromolecules*, 2001, **34**, 4742–4748.

13 M. Jikei and M.-A. Kakimoto, *Prog. Polym. Sci.*, 2001, **26**, 1233–1285.

14 W. Wang, Y. Zheng, E. Roberts, C. J. Duxbury, L. Ding, D. J. Irvine and S. M. Howdle, *Macromolecules*, 2007, **40**, 7184–7194.

15 T. Zhao, Y. Zheng, J. Poly and W. Wang, *Nat. Commun.*, 2013, **4**, 1873–1880.

16 Q. Li, T. Wang, J. Dai, C. Ma, B. Jin and R. Bai, *Chem. Commun.*, 2014, **50**, 3331–3334.

17 J. M. J. Fréchet, M. Henmi, I. Gitsov, S. Aoshima, M. R. Leduc and R. B. Grubbs, *Science*, 1995, **269**, 1080–1083.

18 C. J. Hawker, J. M. J. Fréchet, R. B. Grubbs and J. Dao, *J. Am. Chem. Soc.*, 1995, **117**, 10763–10764.

19 K. Matyjaszewski, S. G. Gaynor and A. H. E. Müller, *Macromolecules*, 1997, **30**, 7034–7041.

20 K. Matyjaszewski, G. S. Gaynor, A. Kulfan and M. Podwika, *Macromolecules*, 1997, **30**, 5192–5194.

21 D. Roy, J. N. Cambre and B. S. Sumerlin, *Chem. Commun.*, 2008, 2477–2479.

22 B. Liu, A. Kazlauciunas, J. T. Guthrie and S. Perrier, *Macromolecules*, 2005, **38**, 2131–2136.

23 J. Bernard, A. Favier, T. P. Davis, C. Barner-Kowollik and M. H. Stenzel, *Polymer*, 2006, **47**, 1073–1080.

24 S. Carter, S. Rimmer, R. Rutkaite, L. Swanson, J. P. A. Fairclough, A. Sturdy and M. Webb, *Biomacromolecules*, 2006, **7**, 1124–1130.

25 S. Hopkins, S. Carter, L. Swanson, S. MacNeil and S. Rimmer, *J. Mater. Chem.*, 2007, **17**, 4022–4027.

26 A. P. Vogt and B. S. Sumerlin, *Macromolecules*, 2008, **41**, 7368–7373.

27 A. Zintchenko, A. Philipp, A. Dehshahri and E. Wagner, *Bioconjugate Chem.*, 2008, **19**, 1448–1455.

28 B. Liang, M.-L. He, Z.-P. Xiao, Y. Li, C.-Y. Chan, H.-F. Kung, X.-T. Shuai and Y. Peng, *Biochem. Biophys. Res. Commun.*, 2008, **367**, 874–880.

29 S. Sun and C. Gao, *Biomacromolecules*, 2010, **11**, 3609–3616.

30 R. K. O'Reilly, *Polym. Int.*, 2010, **59**, 568–573.

31 H. Mori and T. Endo, *Macromol. Rapid Commun.*, 2012, **33**, 1090–1107.

32 S. Filippov, M. Hrubý, Č. Koňák, H. Macková, M. Špírková and P. Štěpánek, *Langmuir*, 2008, **24**, 9295–9301.

33 J. Nicolas, G. Mantovani and D. M. Haddleton, *Macromol. Rapid Commun.*, 2007, **28**, 1083–1111.

34 S. G. Roy, R. Acharya, U. Chatterji and P. De, *Polym. Chem.*, 2013, **4**, 1141–1152.

35 S. Kumar, S. G. Roy and P. De, *Polym. Chem.*, 2012, **3**, 1239–1248.

36 K. Bauri, S. G. Roy, S. Pant and P. De, *Langmuir*, 2013, **29**, 2764–2774.

37 E. Sato, I. Uehara, H. Horibe and A. Matsumoto, *Macromolecules*, 2014, **47**, 937–943.

38 W.-J. Wang, D. Wang, B.-G. Li and S. Zhu, *Macromolecules*, 2010, **43**, 4062–4069.

39 A. B. Lowe and C. L. McCromic, *Prog. Polym. Sci.*, 2007, **32**, 283–351.

40 J. Han, S. Li, S. A. Tang and C. Gao, *Macromolecules*, 2012, **45**, 4966–4977.

41 Z. Wei, X. Hao, P. A. Kambouris, Z. Gan and T. C. Hughes, *Polymer*, 2012, **53**, 1429–1436.

42 D. Yan, A. H. E. Müller and K. Matyjaszewski, *Macromolecules*, 1997, **30**, 7024–7033.

43 Z. Wei, X. Hao, Z. Gan and T. C. Hughes, *J. Polym. Sci., Part A: Polym. Chem.*, 2012, **50**, 2378–2388.

44 G. I. Litvinenko, P. F. W. Simon and A. H. E. Müller, *Macromolecules*, 1999, **32**, 2410–2419.

45 G. I. Litvinenko and A. H. E. Müller, *Macromolecules*, 2002, **35**, 4577–4583.

46 G. I. Litvinenko, P. F. W. Simon and A. H. E. Müller, *Macromolecules*, 2001, **34**, 2418–2426.

47 Z. Wei, X. Hao, Z. Gan and T. C. Hughes, *J. Polym. Sci., Part A: Polym. Chem.*, 2012, **50**, 2378–2388.

48 C. Zhang, Y. Zhou, Q. Liu, S. Li, S. Perrier and Y. Zhao, *Macromolecules*, 2011, **44**, 2034–2049.

49 F. Cheng, E. M. Bonder, A. Doshi and F. Jäkle, *Polym. Chem.*, 2012, **3**, 596–600.

50 A. Narumi, Y. Ohashi, D. Togashi, Y. Saito, Y. Jinbo, Y. Izumi, K. Matsuda, T. Kakuchi and S. Kawaguchi, *J. Polym. Sci., Part A: Polym. Chem.*, 2012, **50**, 3546–3559.

51 Y. Chen, K. Fuchise, A. Narumi, S. Kawaguchi, T. Satoh and T. Kakuchi, *Macromolecules*, 2011, **44**, 9091–9098.

52 X. Xia, Z. Ye, S. Morgan and J. Lu, *Macromolecules*, 2010, **43**, 4889–4901.

53 M. R. Whittaker, C. N. Urbani and M. J. Monteiro, *J. Am. Chem. Soc.*, 2006, **128**, 11360–11361.

54 A. A. Steinschulte, B. Schulte, N. Drude, M. Erberich, C. Herbert, J. Okuda, M. Möller and F. A. Plamper, *Polym. Chem.*, 2013, **4**, 3885–3895.

55 D. Kafouris, M. Gradzielski and C. S. Patrickios, *Macromol. Chem. Phys.*, 2009, **210**, 367–376.

56 D. Kafouris, M. Gradzielski and C. S. Patrickios, *J. Polym. Sci., Part A: Polym. Chem.*, 2008, **46**, 3958–3969.

57 X. Zhu, C. Yan, F. M. Winnik and D. Leckband, *Langmuir*, 2007, **23**, 162–169.

58 S. Kumar, R. Acharya, U. Chatterji and P. De, *Langmuir*, 2013, **29**, 15375–15385.

59 F. A. Plamper, M. Ruppel, A. Schmalz, O. Borisov, M. Ballauff and A. H. E. Müller, *Macromolecules*, 2007, **40**, 8361–8366.

60 M. Luzon, C. Boyer, C. Peinado, T. Corrales, M. Whittaker, L. Tao and T. P. Davis, *J. Polym. Sci., Part A: Polym. Chem.*, 2010, **48**, 2783–2792.

61 K. Bauri, S. Pant, S. G. Roy and P. De, *Polym. Chem.*, 2013, **4**, 4052–4060.

62 G. Wang, H. Yin, J. C. Y. Ng, L. Cai, J. Li, B. Z. Tang and B. Liu, *Polym. Chem.*, 2013, **4**, 5297–5304.

63 A. Kowalczuk, B. Mendrek, I. Żymelka-Miara, M. Libera, A. Marcinkowski, B. Trzebicka, M. Smet and A. Dworak, *Polymer*, 2012, **53**, 5619–5631.

64 S. Lin, F. Du, Y. Wang, S. Ji, D. Liang, L. Yu and Z. Li, *Biomacromolecules*, 2008, **9**, 109–115.

65 K. Bauri, P. De, P. N. Shah, R. Li and R. Faust, *Macromolecules*, 2013, **46**, 5861–5870.

66 Y. Zhou and D. Yan, *Chem. Commun.*, 2009, 1172–1188.

67 D. Roy, W. L. A. Brooks and B. S. Sumerlin, *Chem. Soc. Rev.*, 2013, **42**, 7214–7243.